

Magnetic Dimensionality of Metal Formate $M[(H_2O)_2(HCOO)_2]$ Compounds ($M = \text{Co(II)}, \text{Cu(II)}$)

L. L. L. Sousa^{1,2}, G. F. Barbosa^{1,2}, F. L. A. Machado¹, L. R. S. Araujo^{1,3}, P. Brandão⁴, M. S. Reis⁵, and D. L. Rocco⁵

¹Departamento de Física, Universidade Federal de Pernambuco, 50670-901, Recife, Pernambuco, Brasil

²Departamento de Ciências Exatas e Naturais, Universidade Federal Rural do Semi-Arido, Mossoró, 59.625-900, Rio Grande do Norte, Brasil

³Unidade Acadêmica de Física, Universidade Federal de Campina Grande, 58109-970, Campina Grande, Paraíba, Brasil

⁴Departamento de Química and Centro de Investigação em Materiais Cerâmicos e Compósitos, Universidade de Aveiro, 3810-195, Aveiro, Portugal

⁵Instituto de Física, Universidade Federal Fluminense, 24210-340, Niterói, Rio de Janeiro, Brasil

The magnetic properties of two metal formate systems with formula $M[(H_2O)_2(HCOO)_2]$, which are isostructural, are described ($M = \text{Co}, \text{Cu}$). These compounds contain two different crystallographic metal centers (M^{2+}), in octahedral coordination, which are connected through (HCOO) bridges, leading to the formation of two types of infinite chains: $M(1) - \text{HCOO} - M(2)$ and $M(1) - \text{HCOO} - M(1)$. The packing of these chains, along with hydrogen bonds, generates a 3-D framework. Cu-sample presents an usual paramagnetic behavior, following Curie law. On the contrary, Co-sample has an order-disorder magnetic transition, further analyzed by means of magnetization and specific heat. These data lead us to conclude an anisotropic environment for Co ions, as expected for an octahedral neighborhood. Critical exponents of these thermodynamic quantities around the thermal transition are in accordance with 3-D model. This is a very important remark, since a previous work had shown that the magnetic phase transition is 2-D.

Index Terms—Magnetic materials, magnetic properties, metal formate, structural properties.

I. INTRODUCTION

THE design and synthesis of new molecular magnets with exotic magnetic properties have widely attracted the interest of chemists and physicists in recent years [1], [2]. Zero-dimension (isolated molecule), one-dimension (chains) and higher-dimension structures (2-D and 3-D), exhibit a variety of interesting properties, such as magnetic interaction alternation [3], spin-Peierls transitions [4], Haldane gaps [5], quantum tunneling of the magnetization and other interesting phenomena. These materials are promising to be used in several applications, namely: magnetic recording [6], quantum information/computation [7], [8], spintronics [9] and more. In this sense, the development of new materials and understanding of their physical properties are of crucial importance.

The magnetic properties of $M[(H_2O)_2(HCOO)_2]$ (with $M =$ transition metal) arise from a particular arrangement of magnetic ion (e.g., cobalt, manganese and copper) in the structure. The disposition of magnetic ions generates a crystal structure which is schematically shown in Fig. 1, where it is found that there are two magnetic ions layers (A and B) [10]. Previous studies performed on metal formate systems (with Mn, Fe and Ni ions) [11], [12] had shown that the ions in the A layer (100 plane) have antiferromagnetic (AF) long range order due to an intra-layer interaction; with the formate group acting as an effective intermediary in the superexchange interaction. Ions in the B layer (200 plane) behave paramagnetically even

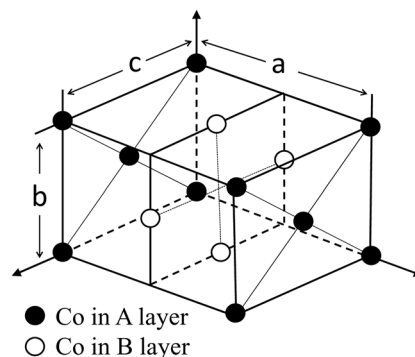


Fig. 1 A schematic representation of arrangement of magnetic ions (for this case, cobalt) in the A and B layers [10].

below T_N of the AF 2-D order above mentioned. According to those papers, the AF transition is only confined in the layer A, since the interaction between A and B layers is quite weak. However, Radhakrishna *et al.* [13, and references therein] had shown that for manganese formate a three-dimensional AF order takes place at 3.7 K, and that two-dimensional AF correlations lies in the $3.7 \text{ K} \leq T \leq 7.8 \text{ K}$ range. The cobalt and copper formate dihydrate systems have already been studied [10], [14] and a two-dimensional AF transition was observed for both compounds.

In order to study the structural and magnetic properties of two metal formates, we prepared, hydrothermally, two compounds with formula $M[(H_2O)_2(HCOO)_2]$ ($M = \text{Co(II)}, \text{Cu(II)}$), which are isostructural [15], [16]. Our goal is to examine, in details, the influence of different spins on the magnetic properties and, by using critical exponents analysis of some thermodynamic quantities, to understand the character of those interactions.

Manuscript received March 12, 2013; revised May 17, 2013; accepted August 06, 2013. Date of publication August 15, 2013; date of current version November 20, 2013. Corresponding author: D. L. Rocco (e-mail: rocco@if.uff.br).

Color versions of one or more of the figures in this paper are available online at <http://ieeexplore.ieee.org>.

Digital Object Identifier 10.1109/TMAG.2013.2278681

TABLE I
PERTINENT CRYSTALLOGRAPHIC DATA FOR $M[(H_2O)_2(HCOO)_2]$ ($M = \text{Co(II)}, \text{Cu(II)}$) AND COMPARISON WITH THE PUBLISHED DATA [15], [16]

	Copper		Cobalt	
	Present work	ref.[15]	Present work	ref.[16]
Empirical formula	$\text{C}_2\text{H}_6\text{CuO}_6$	$\text{C}_2\text{H}_6\text{CuO}_6$	$\text{C}_2\text{H}_6\text{CoO}_6$	$\text{C}_2\text{H}_6\text{CoO}_6$
Formula Weight	189.61		185.00	
Crystal System	Monoclinic	Monoclinic	Monoclinic	Monoclinic
Space group	$P2_1/c$	$P2_1/c$	$P2_1/c$	$P2_1/c$
a (Å)	8.4973(8)	8.54(2)	8.6621(3)	8.68
b (Å)	7.0944(7)	7.15(1)	7.1427(2)	7.06
c (Å)	9.4217(10)	9.59(2)	9.2795(3)	9.21
β ($^\circ$)	97.006(5)	96.8	97.471(2)	96.0
V (Å ³)	563.73(9)	581.45	569.26(3)	558.07
Z	4	4	4	4
D_c [Mg m ⁻³]	2.234		2.159	
Absorpt. correct. (mm ⁻¹)	3.833		2.974	
Crystal size	0.16x0.14x0.02		0.08x0.04x0.02	
Reflections collected	4594		10002	
Unique reflections, [R_{int}]	1508, [0.0202]		1726, [0.0235]	
Final R indices				
R_1, wR_2 [$I > 2\sigma I$]	0.0204, 0.0527		0.0194, 0.0538	
R_1, wR_2 (all data)	0.0262, 0.0603		0.0266, 0.0577	

II. EXPERIMENTAL DETAILS

All reagents were purchased from commercial sources and used without further purification. Synthesis of $\text{Cu}[(\text{H}_2\text{O})_2(\text{HCOO})_2]$: A mixture of $\text{Cu}(\text{CO}_3)\text{Cu}(\text{OH})_2$ (0.60 g, Panreac, assay (as Cu)(Iodom.)55%), formic acid (1.22 g, Merck, 98-100% purity), and 15 ml of distilled water was placed in a 25 ml Teflon-lined stainless steel autoclave, and the vessel was sealed and heated to 110 °C for 24 h, followed by slowly cooling to room temperature. The resulting light blue plated shape crystals were obtained. Synthesis of $\text{Co}[(\text{H}_2\text{O})_2(\text{HCOO})_2]$: The synthesis of the cobalt formate was similar to that of copper formate using instead $2\text{Co}(\text{CO}_3)_3\text{Co}(\text{OH})_2\text{H}_2\text{O}$ (0.019 g, Carlo Erba, assay $50.5 \pm 2.5\%$ Co), as cobalt source. The resulting light pink plated shape crystals were obtained.

A. Single Crystal X-ray Diffraction

The X-ray data were collected on a CCD Bruker APEX II at 150(2) K using graphite monochromatized Mo- $K\alpha$ radiation ($\lambda = 0.71073$ Å). The crystals of copper and cobalt formate compounds were positioned at 35 mm from the CCD and the spots were measured using a counting time of 10 s for copper sample and 30 s for cobalt sample. Data reduction including a multi-scan absorption correction were carried out using the SAINT-NT from Bruker AXS. The structure was refined using full-matrix least squares in SHELXL-97. The C-H and O-H were located from final difference Fourier maps. Anisotropic thermal parameters were used for all non-hydrogen atoms, which were refined with isotropic thermal parameters. The final R values obtained for copper and cobalt samples together with pertinent crystallographic data are summarized in the Table I, and they are comparable with those reported earlier [15], [16]. Molecular diagrams were drawn with PLATON.

B. Thermodynamic Measurements

The ac magnetic susceptibility χ_{ac} was measured from room temperature down to 2 K using a PPMS (Physical Properties Measurement System - Quantum Design). The magnitude and

frequency of the ac magnetic field used to measure the small amount of crystals (5–15 mg) were 10 Oe and 100 Hz, respectively. A home-made extraction magnetometer was used to measure magnetization hysteresis loops above (10 K) and slightly below (5 K) the transition temperature, by varying the applied magnetic field H in the range of ± 1 T. The T -dependence ($2 \leq T \leq 50$ K) of the low magnetic field ($H = 20$ mT) dc magnetic susceptibility (M/H), was measured by the extraction magnetometry. The temperature dependence of the specific heat c_p was also measured using the PPMS. In order to improve the thermal contact within the sample a pellet with approximately 2 mm of diameter and 3.0 mg of mass was made by slightly pressuring the sample. The pellet was then attached to the calorimeter using a small amount (0.4 mg) of N-grease. The addenda (N-grease plus calorimeter) heat capacity was carefully subtracted from the total heat capacity to yield the heat capacity of the sample [17]. It is important to stress that the sample is constituted of small single crystals. However, for thermodynamic measurements, we needed a collection of these crystals and, therefore, for these purpose (magnetization and specific heat), the sample is a powder.

III. CRYSTAL STRUCTURE

As we mentioned above, the crystal structure of $M[(\text{H}_2\text{O})_2(\text{HCOO})_2]$, with $M = \text{Cu(II)}$ and Co(II) , were already published [15], [16]. Therefore, here only a brief description of both structures is present in order to support the understanding of the magnetic results. The asymmetric unit of metal formate complexes is composed of two independent M^{2+} ions, both located on an inversion crystallographic center with occupancy factor of 0.5, and two formate ions $[\text{HCOO}]^-$ and two water molecules with entire occupancies, which is consistent with molecular formula $M[(\text{H}_2\text{O})_2(\text{HCOO})_2]$. Selected distances in the metal coordination sphere are given in Table II. The two independent metal centers are six coordinated exhibiting distorted octahedral coordination environments (Fig. 3). The cobalt metal centers exhibit lesser distorted octahedral coordination environments than copper metal, as indicated by the Co-O distances given in Table II.

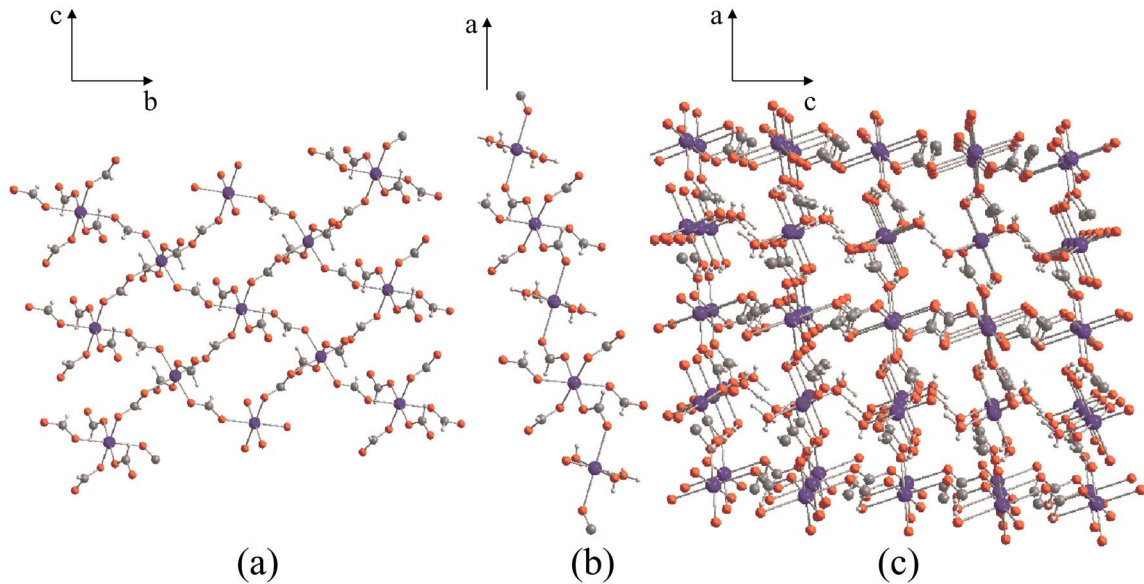


Fig. 2 (a) 2-D layer structure of M(1) ions; b) 1-D chain of M(1)-formate-M(2) ions; c) 3-D structure of $M[(H_2O)_2(HCOO)_2]$ ($M = Co(II)$ and $Cu(II)$) compounds along b direction.

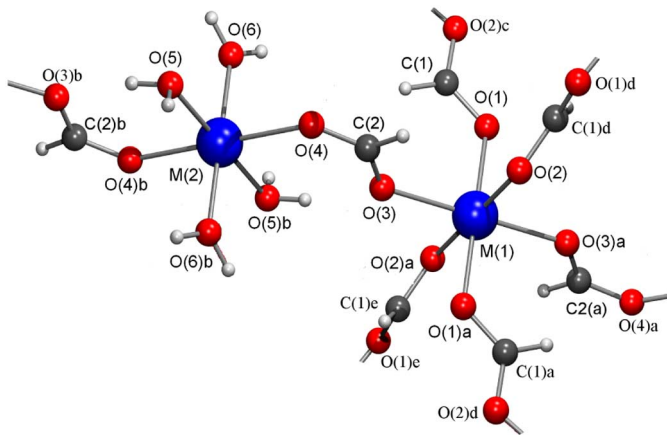


Fig. 3 Octahedral coordination environment of the M(1) and M(2) sites in the metal formate compounds $M[(H_2O)_2(HCOO)_2]$ ($M = Co(II)$ and $Cu(II)$). a denotes the symmetry operation $[-x, -y, 1-z]$, while b means $[1-x, 1-y, 1-z]$.

TABLE II
SELECTED BOND LENGTHS (\AA) IN THE METAL COORDINATION SPHERE OF
 $M[(H_2O)_2(HCOO)_2]$ ($M = Co(II)$ AND $Cu(II)$) COMPOUNDS AND
COMPARISON WITH THE PUBLISHED DATA [15], [16]

Bond angles	Copper		Cobalt	
	Present work	ref.[15]	Present work	ref.[16]
M(1)-O(1)	1.9688(11)	2.025	2.0656(9)	2.038
M(1)-O(2)	2.3370(11)	2.298	2.0949(9)	2.043
M(1)-O(3)	2.0082(11)	2.032	2.1326(9)	2.106
M(2)-O(4)	2.3950(11)	2.353	2.1456(10)	2.063
M(2)-O(5)	1.9454(13)	1.979	2.1205(10)	2.064
M(2)-O(6)	2.0023(13)	2.021	2.0422(10)	2.074

For both compounds, the M-O distances compare well with those reported earlier [15], [16]. The two metal octahedra are bridged via formate ions originating two different infinite chains. One of this chains is built from the infinite linkage of -M(1)-formate-M(1)-formate-M(1)-, with M(1)-M(1) distance of 5.8551 \AA and 5.8964 \AA for Co and Cu, respectively. The

M(1) ions of adjacent chains are further connected to another 1-D chain along the perpendicular direction originating a 2-D layer in the bc plane (Fig. 2(a)), which are the magnetic A layers cited previously in Fig. 1. A second 1-D chain is formed by M(1)-formate-M(2)-formate-M(1)-formate-M(2)-, with M(1)-M(2) distance of 5.6136 \AA and 5.5349 \AA for Co and Cu, respectively (Fig. 2(b)). This 1-D chain is perpendicular to the 2-D layer, leading to the formation of 3-D network structure (Fig. 2(c)). It is interesting to note that the distance M(1)-M(2) gives, indirectly, the distance between A and B layers (Fig. 1), which is smaller than distance M(1)-M(1) (distance between ions in the A layer). In spite of this, as discussed above, the A intra-layer magnetic interaction is stronger than A-B inter-layer.

The cell parameters and the atom coordinate values obtained for the Co and Cu formate solids prepared in our laboratory are comparable with those reported earlier [15], [16].

IV. RESULTS AND DISCUSSION

Both samples have the same structure and therefore the minor differences found on the magnetic behavior came from the spin s of the transition metal M . We measured both, real χ' and imaginary χ'' susceptibilities and found a purely paramagnetic behavior for Cu-sample, without dissipation contribution (signature of a true paramagnetic material). On the contrary, Co-sample has both, dissipation and absorption components, with a quite well defined transition temperature (5.4 K). These first results clearly show that Co ions are turning on a collective magnetic order (long range character), below this transition. Fig. 4 shows these results.

From the same results (AC susceptibility), it is possible to evaluate the modulus $\chi = \sqrt{(\chi')^2 + (\chi'')^2}$ and then its inverse χ^{-1} . For the Cu-sample, we found, as expected, a true paramagnetic character, from high temperature down to the lowest measured. From this behavior, we could fit a straight line to

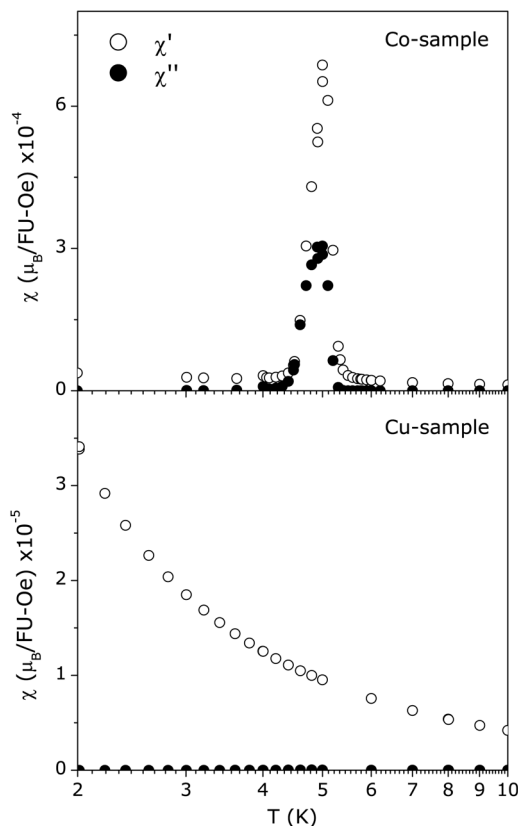


Fig. 4 AC magnetic susceptibility (100 Hz) for both, (above) Co- and (below) Cu-samples.

the data and found the paramagnetic effective moment $p_{eff} = 1.3(1) \mu_B$, while the predicted to Cu^{2+} is

$$p_{eff} = g\sqrt{s(s+1)} = 1.73 \mu_B \quad (1)$$

considering $g = 2$ and $s = 1/2$. This deviation can be an evidence that a fraction of the Cu ions does not contribute to the total magnetic moment. In our calculation we assumed that all the Cu ions were magnetic, while some of them may be at defect positions. In addition to p_{eff} , the paramagnetic Curie temperature was obtained: $\theta_p = -3(1)$ K.

In what concerns Co-sample, the inverse magnetic susceptibility presents a strong deviation from the Curie law, in contrast to the Cu-sample. Since the samples are isostructural, the diamagnetic contribution (temperature independent), is the same for both samples and then it is not the reason for this deviation. Thus, the explanation is a van Vleck temperature independent paramagnetic contribution, that arises from the coupling of the Γ_6 populated level with the excited levels through the Zeeman perturbation, obtained via van Vleck formula [18]. In order to eliminate this temperature independent paramagnetic (TIP) contribution, we dealt with $|d\chi/dT|^{-1/2}$. After this procedure, we found a good straight line, with $p_{eff} = 3.5(6) \mu_B$ and $\theta_p = -23(3)$ K. The magnitude of TIP contribution is of the order of $10^{-8} \mu_B/FU-Oe$ and is commonly found in compounds with Co^{2+} ions in octahedral environment. Fig. 5 clarifies these comments. The paramagnetic effective moment

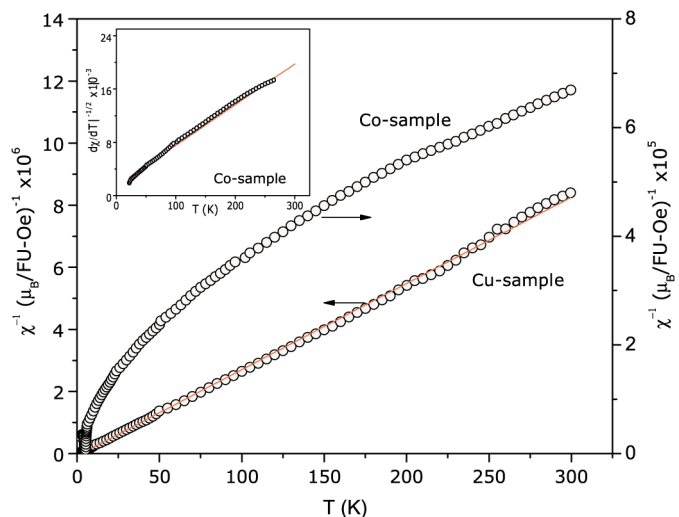


Fig. 5 Inverse magnetic susceptibility for Cu- and Co-sample. Inset: $|d\chi/dT|^{-1/2}$ in order to eliminate any temperature independent magnetic contribution (for Co-sample).

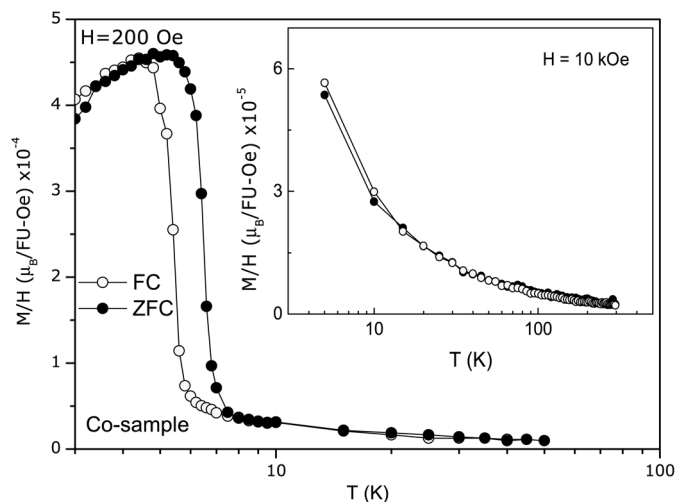


Fig. 6 Zero field cooled (ZFC) and field cooled (FC) magnetic susceptibility for Co-sample. Inset: High field magnetization to show the lost of the thermal irreversibility.

is quite close to the theoretical atomic one: $3.87 \mu_B$, for Co^{2+} ($s = 3/2$). The small deviation (Δp_{eff}) of the measured p_{eff} and the theoretical one ($0.31 \mu_B$) is comparable to the one ($0.42 \mu_B$) observed for the Cu sample. The negative value of θ_p is an indicative of an antiferromagnetic arrangement between Co ions. The low values (for both samples), of θ_p , is in agreement with syn-anti conformation (see Fig. 3 and reference [8]).

In order to extend our understanding on the magnetic properties of Co-sample, we go further and measured some other quantities, namely magnetization and specific heat. A small thermal hysteresis was observed while measuring zero-field cooled and field cooled magnetization under low magnetic field, as seen at the main picture of Fig. 6. It is important to stress that this hysteresis vanishes for higher values of applied magnetic field (10 kOe—see inset of that figure). We can understand this result from the $M(H)$ curve: note that the sample is in a magnetic

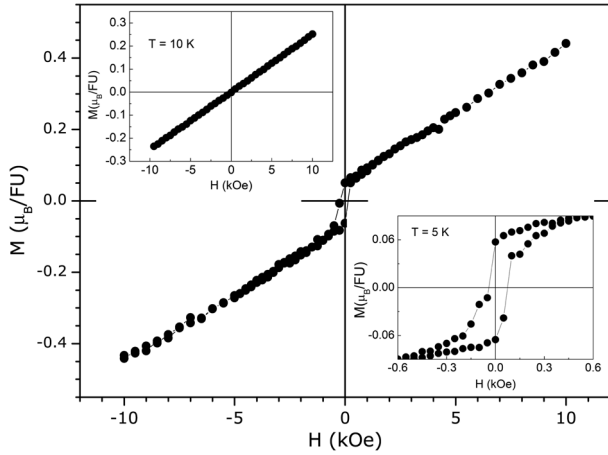


Fig. 7 Magnetization above and below the critical temperature (5.0 K), for Co-sample. Main figure: 5 K. Right inset: details of the main figure around zero field. Left inset: 10 K.

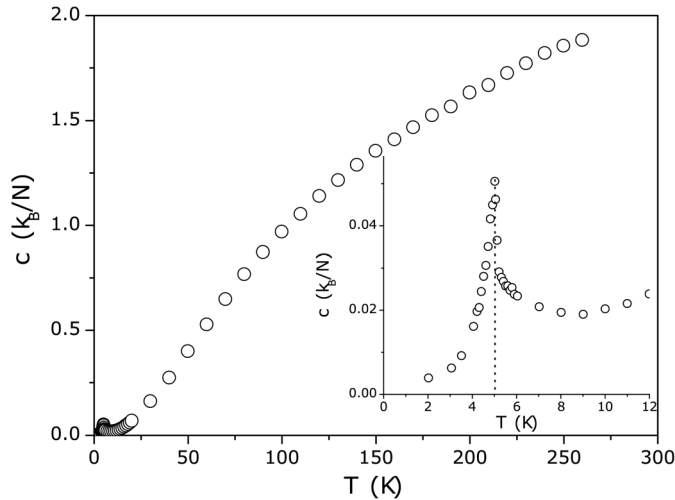


Fig. 8 Specific heat for Co-sample. Inset: details around the transition.

hysteretic regime at low value of magnetic field, while it is not for higher values (see Fig. 7).

Magnetization as a function of magnetic field (Fig. 7), presents a linear behavior above 5.0 K, due to the paramagnetic behavior; while below this critical temperature we found a well defined hysteresis loop and linear tendency out of this loop, as an indicative of the antiferromagnetic character. This behavior can be a signature of a spin canting of Co ions; the ferromagnetic component provides the hysteresis, while the antiferromagnetic component provides the linear background. This kind of behavior is found in anisotropic systems, with anti-symmetric-like interactions.

Finally, specific heat measurements (Fig. 8) present an evident Debye behavior (main figure) with a lambda-like transition around the critical temperature (bottom inset).

Considering a reduced temperature.

$$t = \frac{T}{T_c} - 1 \quad (2)$$

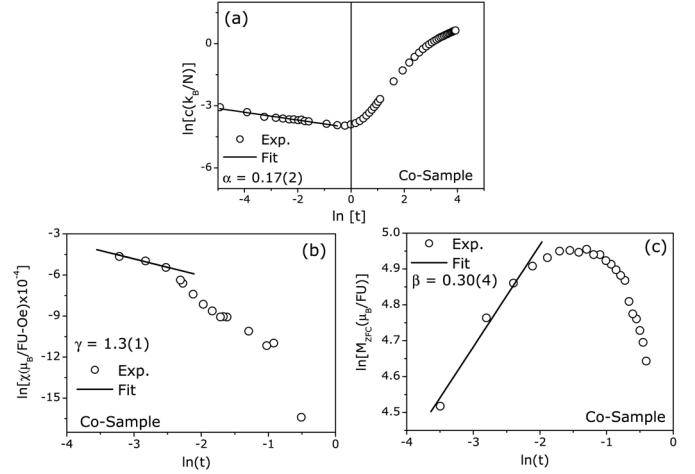


Fig. 9 Logarithm of the (a) specific heat, (b) AC magnetic susceptibility and (c) ZFC magnetization as a function of the logarithm of the reduced temperature (equation 2), to obtain the critical exponents α , γ and β , respectively.

TABLE III
EXPERIMENTAL AND THEORETICAL CRITICAL EXPONENTS FOR SOME THERMODYNAMIC QUANTITIES. MFT - MEAN FIELD THEORY; I2D - ISING 2D; H3D - HEISENBERG 3D; I3D - ISING 3D

	MFT	I2D	H3D	I3D	exp.
α	0	0	0.14	0.11	0.17(2)
β	1/2	1/8	0.3	0.33	0.30(4)
γ	1	7/4	1.4	1.24	1.3(1)

we proceed an analysis based on the critical exponents of those thermodynamic quantities [6], [19]:

$$c \sim |t|^{-\alpha} \quad (3)$$

$$M \sim |t|^{\beta} \quad (4)$$

$$\chi \sim |t|^{-\gamma} \quad (5)$$

as shown in Fig. 9. Analysis was performed to three quantities slightly below the transition temperature and the results are summarized on Table III, where it is also possible to find the predicted critical exponents of some theoretical models. From this comparison, we can argue that this material follows a 3-D model, as suggested in our structural analysis. The octahedral environment of Co ions suggests an anisotropic character and indeed we found this signature on $M(H)$ curves. The critical exponents point towards a 3-D character below the transition, but it is difficult to determine, only from these values, between H3D (Heisenberg 3D) and I3D (Ising 3D—highly anisotropic). However, the previous discussion of the hysteresis clarifies this anisotropic tendency of those ions.

V. CONCLUSION

In summary, two molecular compounds, namely, $M[(\text{H}_2\text{O})_2(\text{HCOO})_2]$ ($M = \text{Co}, \text{Cu}$), were prepared and their thermodynamic quantities were investigated by means of magnetization, magnetic susceptibility and heat

capacity measurements. The material with Cu was found to be paramagnetic in the range of investigated temperatures in the present work. However, a rather sharp magnetic phase transition below 5.0 K was observed in the isostructural Co-based material. The overall magnetic behavior was found to be consistent with the proposed atomic structure and the critical exponents associated to the phase transition indicated that the magnetic phase transition is 3-D and anisotropic in character. This is a very important remark, since a previous study [14] had shown that the magnetic phase transition is 2-D. We found that the three-dimensional AF arrangement takes place at higher temperature than that one observed for Mn formate [13]. The reason is that the exchange parameter between A and B layers for Co formate is twice larger than for Mn formate [14].

ACKNOWLEDGMENT

This work was supported in part by PROPPi - UFF, CNPq, CAPES, FINEP, FACEPE and FAPERJ (Brazilian Agencies).

REFERENCES

- [1] S. J. Blundell and F. L. Pratt, "Organic and molecular magnets," *J. Phys.: Condens. Matter*, vol. 16, p. R771, 2004.
- [2] B. Sougato, "Quantum communication through spin chain dynamics: an introductory overview," *Contemp. Phys.*, vol. 48, p. 13, 2007.
- [3] P. Brandão, F. Paz, and J. Rocha, "A novel microporous copper silicate: $\text{Na}_2\text{Cu}_2\text{Si}_4\text{O}_{11.2}\text{H}_2\text{O}$," *Chem. Comm.*, vol. 2, p. 171, 2005.
- [4] M. Hase, I. Terasaki, and K. Uchinokura, "Observation of the spin-Peierls transition in linear Cu^{2+} (spin-1/2) chains in an inorganic compound CuGeO_3 ," *Phys. Rev. Lett.*, vol. 70, p. 3651, 1993.
- [5] M. Yamashita, T. Ishii, and H. Matsuzaka, "Haldane gap systems," *Coor. Chem. Rev.*, vol. 198, p. 347, 2000.

- [6] Z. L. Huang, M. Drillon, N. Masciocchi, A. Sironi, J. T. Zhao, P. Rabu, and P. Panissod, "Ab-initio XRPD crystal structure and giant hysteretic effect ($H_c = 5.9$ T) of a new hybrid terephthalate-based cobalt(II) magnet," *Chem. Mat.*, vol. 12, no. 9, p. 2805, 2000.
- [7] A. M. Souza, M. S. Reis, D. O. Soares-Pinto, I. S. Oliveira, and R. S. Sarthour, "Experimental determination of thermal entanglement in spin clusters using magnetic susceptibility measurements," *Phys. Rev. B*, vol. 77, p. 104402, 2008.
- [8] A. M. Souza, D. O. Soares-Pinto, R. S. Sarthour, I. S. Oliveira, M. S. Reis, P. Brandão, and A. M. dos Santos, "Entanglement and Bell's inequality violation above room temperature in metal carboxyla," *Phys. Rev. B*, vol. 79, p. 054408, 2009.
- [9] L. Bogani and W. Wernsdorfer, "Molecular spintronics using single-molecule magnets," *Nature Mater.*, vol. 7, p. 179, 2008.
- [10] M. Matsuura, K. Takeda, T. Satoh, and Y. Sawada, "Heat capacity and magnetic interactions in copper formate dihydrate," *Solid State Commun.*, vol. 13, p. 467, 1973.
- [11] R. D. Pierce and S. A. Friedberg, "Heat capacity of $\text{Mn}(\text{HCOO})_{2.2}\text{H}_2\text{O}$ and $\text{Ni}(\text{HCOO})_{2.2}\text{H}_2\text{O}$ 1.4 and 20°K," *Phys. Rev.*, vol. 165, p. 680, 1968.
- [12] R. D. Pierce and S. A. Friedberg, "Heat capacities of $\text{Fe}(\text{HCOO})_{2.2}\text{H}_2\text{O}$ and $\text{Ni}(\text{HCOO})_{2.2}\text{H}_2\text{O}$ between 1.4 and 20 °K," *Phys. Rev. B*, vol. 3, p. 934, 1971.
- [13] P. Radhakrishna, B. Gillon, and G. Chevrier, "Superexchange in manganese formate dihydrate, studied by polarized-neutron diffraction," *J. Phys. Condens. Matter*, vol. 5, p. 6447, 1993.
- [14] K. Takeda, T. Haseda, and M. Matsuura, "A study of magnetic phase transition in a two-dimensional lattice by heat capacity measurements," *Physica*, vol. 52, p. 225, 1971.
- [15] M. Bukowska-Strzyzewska, "The crystal structure of copper(II) formate dihydrate," *Acta Crystallogr.*, vol. 19, p. 357, 1965.
- [16] A. S. Antsyshkina, M. K. Gusejnova, and M. A. Porai-Koshits, "Crystal structure of cobalt formate dihydrate," *Zh. Strukt. Khim.(Russ.)(J. Struct. Chem.)*, vol. 8, p. 321, 1967.
- [17] F. L. A. Machado and W. G. Clark, "Ripple method: An application of the square-wave excitation method for heat-capacity measurements," *Rev. Sci. Instrum.*, vol. 59, p. 1176, 1998.
- [18] O. Khan, *Molecular Magnetism*. VHC, Inc.: , 1942.
- [19] M. Kolesik and M. Suzuki, "Accurate estimates of 3D Ising critical exponents using the coherent-anomaly method," *Physica A*, vol. 215, p. 138, 1995.